Zygote

cambridge.org/zyg

Micromorphological and ultrastructural description of spermatozoa from squirrel monkeys (*Saimiri collinsi* Osgood, 1916)

Danuza L. Leão[1,2], Wlaisa V. Sampaio[1,2,3], Patrícia C. Sousa[1], Arlindo A.A. Moura[4], Irma C. Oskam[5,6], Regiane R. Santos[1] and Sheyla F.S. Domingues[1,2,5,6]

[1]Laboratory of Wild Animal Biotechnology and Medicine, Federal University of Pará, Belém, Pará, Brazil; [2]Post graduation programme in Animal Health and Production in the Amazon, Federal Rural University of the Amazon, Belém, Pará, Brazil; [3]Federal Rural University of the Amazon, Campus Parauapebas, Pará, Brazil; [4]Laboratory of Animal Physiology, Federal University of Ceará, Ceará, Brazil; [5]The Animal Production Experimental Center, Norwegian University of Life Sciences, Ås, Norway and [6]Faculty of Veterinary Medicine, Federal University of Pará, Castanhal, Pará, Brazil

Research Article

Cite this article: Leão DL *et al.* (2020) Micromorphological and ultrastructural description of spermatozoa from squirrel monkeys (*Saimiri collinsi* Osgood, 1916). *Zygote*. **28**: 203–207. doi: 10.1017/S0967199419000868

Received: 20 August 2019
Revised: 30 October 2019
Accepted: 5 December 2019
First published online: 14 January 2020

Keywords:
Electron microscopy; Neotropical primates; Scanning; Sperm; Transmission

Author for correspondence:
Danuza Leite Leão. Laboratory of Wild Animal Biotechnology and Medicine, Federal University of Pará, BR 316 Km 61, CEP 68740-970, Castanhal, Pará, Brazil. Tel: +55 91 33114707. E-mail: danleao.88@gmail.com

Summary

Saimiri collinsi is used as an animal model in biotechnology research for conservation of species from the genus *Saimiri*. However, the development of biotechnologies depends on a proper knowledge of the sperm morphology to understand the basic aspects of sperm physiology, as potential male fertility depends on different cellular sperm structures. With this purpose, this study characterized the micromorphological and ultrastructural characteristics of squirrel monkeys (*Saimiri collinsi*) sperm using scanning electron microscopy (SEM) and transmission electron microscopy (TEM). SEM electromyography revealed that a normal *Saimiri collinsi* sperm measures 71.7 ± 0.7 µm with lateral tail insertion, a paddle-shaped flattened head and an acrosome occupying most of the head. TEM also showed that the middle piece is characterized by a central 9 + 2 microtubule axoneme surrounded by nine dense fibres, and that the mitochondria were juxtaposed, forming the mitochondrial sheath. Here we provide the first micromorphological and ultrastructure description of *S. collinsi* sperm.

Introduction

The squirrel monkey *Saimiri collinsi*, a neotropical primate endemic from the Amazon region of Brazil, is used as an animal model for conservational and biotechnology studies for species from the genus *Saimiri* (Oliveira *et al.*, 2015, 2016a, 2016b). Among these, *S. oerstedii* and *S. vanzolini* are listed as vulnerable, while *S. ustus* is almost threatened to extinction (IUCN, 2019).

Despite the relevant studies conducted to investigate the male reproductive physiology in this non-human primate using classical semen analysis (Oliveira *et al.*, 2015, 2016a, 2016b; Sampaio *et al.*, 2017; Almeida *et al.*, 2018), knowledge on the morphology of sperm from *S. collinsi* is still limited. Seminal analysis or spermiogram is an important tool to evaluate and determine sperm morphological aspects that are directly related to potential male fertility (Visco *et al.*, 2010) and is crucial for the processes of artificial insemination, *in vitro* fertilization, and embryo development (Ozkavukcu *et al.*, 2008).

At a routine basis, sperm morphology from neotropical primates has been examined in semen smears with the main criteria for normality relying on morphological parameters of the sperm head, middle piece and flagellum (Leão *et al.*, 2015; Oliveira *et al.*, 2015, 2016a, 2016b; Swanson *et al.*, 2016; Arakaki *et al.*, 2017, 2019; Sampaio *et al.*, 2017). In *S. collinsi*, sperm morphology has only been described by optical microscopy using eosin–nigrosine staining (Oliveira *et al.*, 2015, 2016a, 2016b; Sampaio *et al.*, 2017). However, sperm analysis using optical microscopy has low resolution, and does not allow the identification and analysis in more detail than at the micro-anatomical level that can affect the sperm and decrease sperm capacity to fertilize the oocyte (Visco *et al.*, 2010).

In this context, the scanning electron microscopy (SEM) and transmission electron microscopy (TEM) are technologies that provide a high-range view, on the nanometre scale, that can aid morphological description and detection of possible abnormalities in the sperm (Nussdorfer *et al.*, 2018). These techniques have already been used in domestic animals such as horses (Pesch *et al.*, 2006), sheep (López-Armengol *et al.*, 2012), and wild animals such as the six-banded armadillo (Sousa *et al.*, 2013), collared peccaries (Bezerra *et al.*, 2018), jaguar (Silva *et al.*, 2019) and some non-human primates (Bedford and Nicander, 1971; Martin *et al.*, 1975; Gould, 1980; Steinberg *et al.*, 2009; Nakazato *et al.*, 2015). For these microscopy technologies in the genus *Saimiri*, only SEM has been used to characterize sperm morphology in squirrel monkeys (*S. sciureus*) (Martin *et al.*, 1975; Gould, 1980), or obtain morphometric sperm data

CAMBRIDGE UNIVERSITY PRESS

as a tool for more accurate taxonomic identification of the *S. boliviensis* (Steinberg *et al.*, 2009). In *S. collinsi* nothing is known about sperm components in higher resolution. Therefore, the aim of the present study was to describe the micro-morphological and ultrastructural characteristics of squirrel monkeys (*S. collinsi*) sperm using SEM and TEM.

Materials and methods

Study facilities

Semen collection was carried out at the National Primate Center (CENP, Ananindeua, Pará, Brazil), SEM was conducted at the Analytical Center of the Universidade Federal do Ceará (UFC, Fortaleza, Ceará, Brazil), and transmission electron microscopy was conducted at the Laboratory of Electron Microscopy of the Evandro Chagas Institute (IEC, Belém, Pará, Brazil).

Animals and semen collection

Saimiri collinsi males originated from the Marajó Archipelago (0°58′S and 49°34′W) and maintained in captivity at the CENP (1°22′58′′S and 48°22′51′′W) and were used for collecting semen. The experimental group ($n = 5$ males, *c.* 15 years old) was selected by their physical characteristics, and clinical parameters such as complete haemogram, hepatic and renal function.

Animals were collectively housed in mixed groups (males and females in a varied number of members) in cages of 4.74 m × 1.45 m × 2.26 m (length, width and height, respectively), under natural photoperiod (i.e. 12 h of light and 12 h of dark). The climate is humid and tropical, with an average annual temperature of 28°C. The diet consisted of fresh fruits, vegetables, commercial pellet chow specific for neotropical non-human primates (Megazoo® P18, 18% protein, 6.5% fibre, Brazil) and cricket larvae (*Zophobas morio*). Vitamins, minerals and eggs were supplied once a week, and water was available *ad libitum*.

Semen collection

Semen was collected at the same period of the day (in the morning before feeding). Physical restraint was performed by a trained animal caretaker wearing leather gloves. All animals were anaesthetized with ketamine hydrochloride (20 mg/kg intramuscularly (IM); Vetanarcol, König S.A., Avellaneda, Argentina) and xylazine hydrochloride 1 mg/kg IM; Kensol, König S.A.), and monitored by a veterinarian.

Achieved total anaesthetic effect, the animals were placed in lateral recumbency, genital region was then sanitized with a mild soap and distilled water (1:10) and gauze. The prepuce was retracted with the thumb and index fingers for a more efficient cleaning of the penis with saline solution. Animals were stimulated with rectal electroejaculation (EEJ) procedure described by Oliveira *et al.* (2015). Ejaculates (liquid and coagulated fractions) were collected into microtubes (1.5 ml), then were placed in a water bath at 37°C. SEM and TEM were only performed in the liquid fraction of the ejaculate.

Sperm preparation

The sample (liquid fraction) were centrifuged at 500 g for 5 min, and the supernatant was discarded. Centrifugation was performed due to the low sperm concentration in the liquid fraction, and to remove the seminal plasma. The pellet formed was washed three times in sodium cacodylate and placed in Karnovsky fixative (4% paraformaldehyde, 2.5% glutaraldehyde in 0.1 M sodium cacodylate buffer, pH 7.2).

Semen evaluation

Seminal volume (liquid fractions) was evaluated in a graduated tube, with the aid of a pipette. Appearance and consistency were assessed subjectively, that is colour (colourless, yellowish, or whitish) and opacity (opaque or transparent) (Oliveira *et al.*, 2015). Sperm motility, vigour, and morphology were evaluated according to Oliveira *et al.* (2015, 2016a, 2016b). Sperm morphology and plasma membrane integrity were evaluated using a prepared smear, adding 5 µl eosin 1% (Vetec) and 5 µl nigrosine 1% (Vetec) to 5 µl of semen on a pre-warmed (37°C) glass slide. Sperm concentration was determined in a Neubauer chamber after dilution of 1 µl semen in 99 µl formalin solution 10%. Morphologic defects detected in sperm were classified as primary or secondary according Bloom (1973). Plasma membrane functionality was assessed by hypoosmotic swelling test (HOST) after dilution of 5 µl of semen in 45 µl of hypoosmotic solution (0.73 g sodium citrate, 1.35 g fructose and 100 ml ultrapure water; pH 7.2 and 108 mOsm/l). After 45 min incubation in a water bath (37°C), number of sperm tail coiled was assessed by placing 10 µl of this solution on a pre-warmed (37°C) glass slide with coverslip, and at least 200 spermatozoa were counted. Spermatozoa with functional plasma membrane were those presenting a coiled tail. All evaluations were performed under a light microscope (Nikon E400, Japan) at a magnification of ×100.

Scanning electron microscopy

Sperm samples were placed in a coated coverslip with poly-D-lysine, air-dried it onto a filter and dehydrated in a series of acetone solution (50, 70, 90 and 100% × 3 or 5 min each). Afterwards, the samples were dried using the critical point method (EMS 850, Quorum Technologies, Lewes, UK) and then attached to supports using aluminium stubs with carbon tape. The samples were covered with a thin (20 nm) layer of gold (Q150T ES, Quorum Technologies, Lewes, UK) and observed under SEM (Quanta 450-FEG, Thermo Fisher Scientific, Massachusetts, USA). The description of *S. collinsi* sperm by SEM was conducted according to that previously reported for non-humans primates by Martin *et al.* (1975).

Transmission electron microscopy

For TEM, the sperm sample were washed in 0.05 M cacodylate buffer (40 min, three times), post-fixed with osmium tetroxide (OsO4) for 60 min and washed in 0.05 M cacodylate buffer with 0.08% potassium ferrocyanide (40 min, five times). Subsequently, the contracting block was performed using 2.5% uranyl acetate in 50% acetone for 1 h. Then, the samples were dehydrated in a series of acetone solutions (70, 80, 90 and 100%) for 10 min each, the solution of 100% acetone was carried out three times. After dehydration, the samples were infiltrated with epoxy resin (EponPolibed), using an increasing series of resin in acetone (dilution 1:2; 1:1; 2:1), until 100% Epon + 2,4,6-trisdimethylaminomethylphenol (DMP-30). Polymerization of the resin was performed at 60°C for 48 h. Semithin cuts of *c.* 70 nm thickness were obtained using an ultramicrotome with glass cutters (Leica EM UC7, Leica Microsystems, Wetzlar, Germany) and contrasted with 5% uranyl acetate for 20 min in 60°C. Observations of the sperm ultrastructure were performed using TEM (EM 900, Carl Zeiss, Brasil Ltd, São Paulo, Brazil).

https://doi.org/10.1017/S0967199419000868 Published online by Cambridge University Press

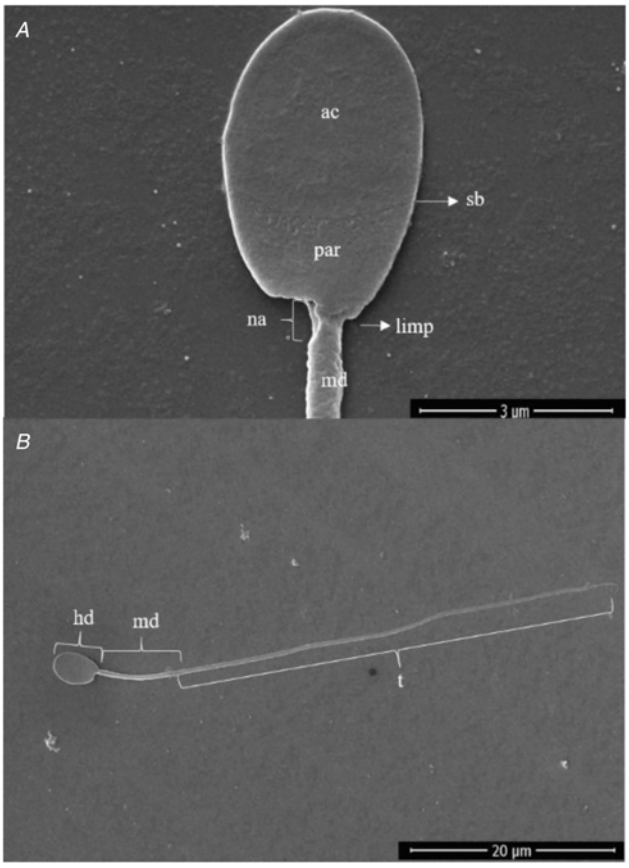

Figure 1. Scanning electron micrographs of *Saimiri collinsi* sperm. (*A*) Sperm head with plasma membrane integrity, acrosomal region (ac), serrated band (sb); post-acrosomal region (par), neck area (na), lateral insertion of the middle piece (limp) and middle piece (md). (*B*) Normal sperm: head (hd), middle piece (md) and tail (t).

Results

Semen evaluation

Mean (± standard error of the mean) of seminal volume was 339 ± 61 µl (15–500 µl; min–max). Liquid fractions were whitish or yellowish, and opaque. Sperm concentration was $1.718 \pm 610 \times 10^6$ sperm/ml. In addition, the samples presented a mean of 67 ± 11% motility, 3 ± 0.3 vigour, 38 ± 13% and 43 ± 8% functional and intact sperm membranes, respectively. Evaluation of sperm morphology through light microscopy was 56 ± 5% normal sperm, 13 ± 4 bent tail, 27 ± 4 coiled tail and 3.6 ± 1.2 strongly coiled tail.

Scanning electron microscopy

SEM revealed that the head of *S. collinsi* sperm was a flattened paddle-shaped with a uniform thickness throughout, measuring 5.14 ± 0.08 µm in length and 3.36 ± 0.03 µm in width, with an intact and uninterrupted surface. The acrosome occupied most of the head with length of 3.56 ± 0.06 µm (Fig. 1*A*). The insertion of the tail was lateral (abaxial; Fig. 1*A*), with length of middle piece at 9.49 ± 0.38 µm. The squirrel monkey sperm presented a total length of 71.7 ± 0.7 µm (Fig. 1*B*).

Transmission electron microscopy

TEM images showed the *S. collinsi* sperm presents a flattened head in a longitudinal cut, containing a very electron-dense nucleus, which is larger at the base, narrowing as it goes to the tip of the head. There is a diffuse small electronic spot. The structures present in the sperm head are the nucleus, the acrosome, and membranous envelopes (Fig. 2*A, B*). The large nucleus is covered by the acrosome (ac), which occupies one-half to two-thirds of the anterior portion of the head. The acrosome is thickest around the anterior margin of the sperm head, and thinnest from the

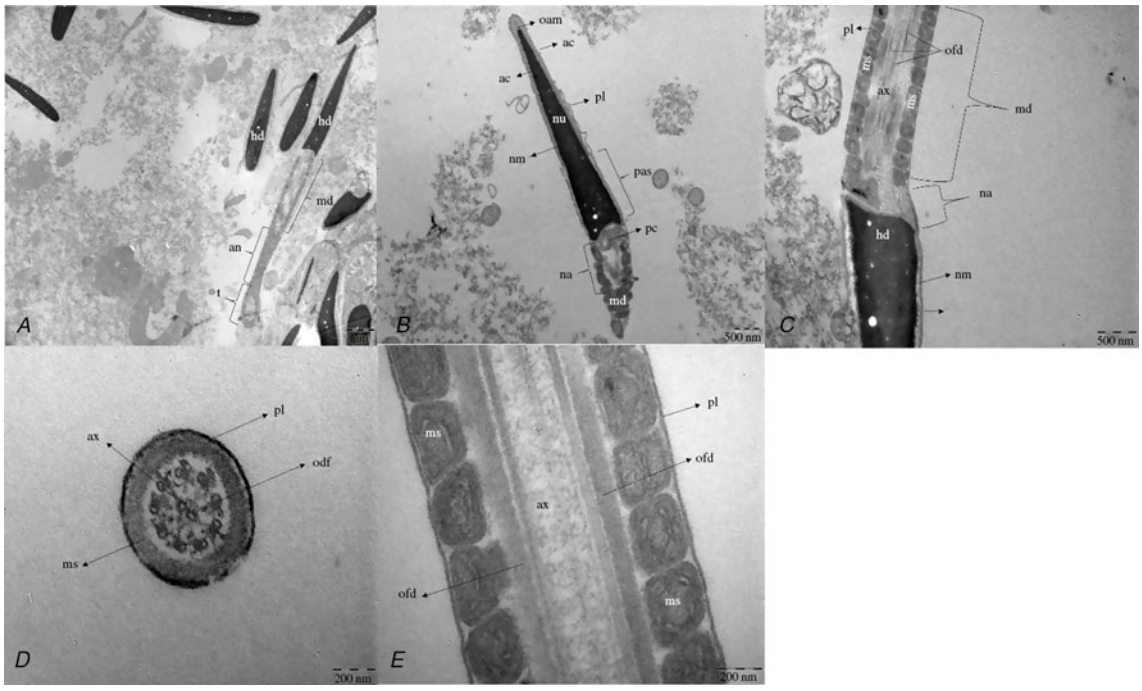

Figure 2. Transmission electron micrographs of the squirrel monkey (*Saimiri collinsi*) sperm. (*A*) hd: head; md: middle piece; an: annulus; t: tail. (*B*) oam: outer acrosome membrane; ac: acrosome; pl: plasmalemma; nu: nucleus; nm: nuclear membrane; pas: postacrosomal sheath; pc: principal centriole: na: neck area; md: middle piece. (*C*) pl: plasmalemma; nm: nuclear membrane: hd: head; na: neck area; md: middle piece; ax: axonema; ofd: outer dense fibres; ms: mitochondrial spiral. (*D*) pl: plasmalemma; ax: axonema; odf: outer dense fibres; ms: mitochondrial spiral; *: longitudinal cut. (*E*) ofd: outer dense fibres; ax: axonema; pl: plasmalemma, ms: mitochondrial spiral.

https://doi.org/10.1017/S0967199419000868 Published online by Cambridge University Press

equator to the posterior third of the nucleus where it terminates (Fig. 2*B*). The neck area (na), which is the region located between the head and the middle piece, is characterized by the presence of a centriole, the proximal centriole (oriented transversally to the cell; pc), and segmented columns (Fig. 2*B*). The middle piece is characterized by a central 9 + 2 microtubule axoneme surrounded by nine dense fibres. This set is surrounded by a plasmalemma and a helical mitochondrial sheath (Fig. 2*C, D*), which identified the presence of an intact axoneme as well as outer dense fibres. The mitochondria were juxtaposed, therefore forming the mitochondrial sheath, which was surrounded by the plasmalemma with some undulations (Fig. 2*E*). It was possible to visualize about *c.* 72 mitochondria.

Discussion

Our study represents a valuable basis for understanding sperm physiology through the description of micromorphological and ultrastructural aspects in *S. collinsi*. Evaluation of sperm morphology has become much more precise, and rigorous analysis of these parameters is of pivotal importance in semen, as it permits detailed study of different sperm abnormalities that predict the fertile capacity of the male gamete (WHO, 2010).

In the genus *Saimiri*, SEM has been performed only in *S. sciureus* (Martin *et al.*, 1975) and *S. boliviensis* (Steinberg *et al.*, 2009). In *S. collinsi*, the abaxial tail insertion was also observed by SEM, as previously described as a normal morphology characteristic in the morphometric analysis of sperm stained with eosin–nigrosine for *S. collinsi* and *S. vanzolini* (Sampaio *et al.*, 2017). The average total length of the *S. collinsi* sperm was similar to that described for other squirrel monkeys species in stained samples (Nakazato *et al.*, 2015; Sampaio *et al.*, 2017). The morphology of the sperm head showed a thick, flattened, paddle-shape that resembled that in other primates, including humans (Martin *et al.*, 1975; Gould & Martin, 1978). The measurements of head morphology for *S. collinsi* using SEM agreed with values obtained previously via optical microscopy (Sampaio *et al.*, 2017).

For the first time, an ultrastructure description of *S. collinsi* sperm by TEM was reported. Therefore, the results presented here will serve as a parameter for future morphological studies involving the preparation and evaluation of semen in non-human primates, as well as for studies using morphological data for the diagnosis of sperm changes, including acquired damage post-thawing, which is a relevant factor for development of reproduction (reproductive) biotechnology (Sousa *et al.*, 2013). TEM might be an additional diagnostic tool for the presence of asthenozoospermia or the absence of motility, which is important as the pattern of axoneme structure can be visualized in longitudinal sections and cross-sections using this technique. In humans, TEM has been used to diagnose sperm changes that have a possible genetic origin, known as systematic defects (Baccetti *et al.*, 2001). The observation of sperm head ultrastructure revealed a large and obvious nucleus. The acrosome is the only cytoplasmic element in the sperm head. Similar to that described for human sperm, in *S. collinsi*, the acrosome was a relatively inconspicuous and covers the anterior two-thirds to one-half of the head, cap-like structure containing enzymes that are essential for fertilization (Bartoov *et al.*, 1980). In Rhesus monkeys sperm, the acrosome is thickest around the anterior margin of the sperm head and thinnest from the equator to the posterior third of the nucleus, where it terminates. The thin portion of the acrosome is usually referred to as the equatorial segment. As shown in human and Rhesus monkey (Zamboni *et al.*,1971), in *S. collinsi* the plasma membrane surrounding the anterior portion of the head is continuous and often undulated.

The sperm head and tail are connected via the sperm neck, a region formed by the centriole and connecting piece (Bornens, 2012). In Rhesus macaque, the middle piece sheath consists of 84–86 mitochondria (Zamboni *et al.*, 1971). In our study, the exact number of mitochondria in *S. collinsi* could not be measured due to the absence of longitudinal sections showing the middle piece to its full extent. These organelles function to provide energy for movement of the flagella, as the midpiece accommodates more mitochondria to produce more energy to fuel motility (Pesch *et al.*, 2006), and generates greater propulsion forces in the principal piece (Gomendio and Roldan, 1991). However, it has been demonstrated that swimming speed is not dependent on the tail size, but on head size, which in return may retard the propulsion generated by the sperm tail (Humphries *et al.*, 2008).

Regarding morphological defects found using light microscopy, according to Bloom (1973) classification, some secondary defects were identified in the *S. collinsi* sperm, including bent tail, coiled tail and strongly coiled tail. Such defects have also been verified in the ejaculates of neotropical primates (Leão *et al.*, 2015; Oliveira *et al.*, 2015; Swanson *et al.*, 2016; Arakaki *et al.*, 2017, 2019). Comparing our study with others already carried out for *S. collinsi* species (Oliveira *et al.*, 2015, 2016a, 2016b; Sampaio *et al.*, 2017), we observed a high percentage of sperm pathologies, which Sampaio *et al.* (2017) characterized as a group of animals with low seminal quality. Conversely, it is noteworthy that we only worked with the liquid fraction for sperm characterization, as the dilution process could generate changes in sperm morphology. It is known that the liquid fraction is the fraction of lower seminal volume and sperm concentration (Oliveira *et al.*, 2015), and may also contain sperm with higher percentages of sperm pathologies when compared with the coagulated fraction.

Saimiri collinsi ejaculates presented a normal range for sperm morphology similar to that accepted for the genus *Saimiri*. Additionally, they presented a general sperm structure, but with characteristics such as an abaxial middle piece insertion, seen using SEM.

Acknowledgements. We would also like to thank to the National Primate Center (CENP/Brazil), to Central Analytical of the Federal University of Ceará and Laboratory of Electronic Microscopy of Evandro Chagas Institute for the technical support during this research.

Financial support. The authors thank 'Coordenação de Aperfeiçoamento de Pessoal de Nível Superior – Brasil (CAPES) – Finance Code 001, and 'Conselho Nacional de Desenvolvimento Científico e Tecnológico (Projeto Universal 01-2016/ Processo no. 421649/2016-0)' for financial support.

Conflicts of interest. The authors declare that there is no conflict of interest that can be perceived as prejudicing the impartiality of the research reported.

Ethical standards. This study was approved by the Ethical Committee in Animal Research (no. 02/2015/CEPAN/IEC/SVS/MS) and by the System of Authorization and Information in Biodiversity (SISBIO/ICMBio/MMA no. 47051-2). All procedures were performed under the supervision of a veterinarian.

References

Almeida DVC, Lima JS, Leão DL, Oliveira KG, Santos RR, Domingues SFS and Miranda MS (2018) The effects of Trolox on the quality of sperm from captive squirrel monkey during liquefaction in the extender ACP-118™. *Zygote* **26**, 333–35.

https://doi.org/10.1017/S0967199419000868 Published online by Cambridge University Press

Arakaki PR, Carvalho FM, Castro PHG, Muniz JAPC and Valle RDRD (2017) Collection, evaluation, and coagulum dissolution of semen from Goeldi's monkey, *Callimico goeldii*. *Folia Primatol* **88**, 334–43.

Arakaki PR, Nichi M, Monteiro FOB, Muniz JAPC, Guimarães MABV and Valle RDRD (2019) Comparison of semen characteristics and sperm cryopreservation in common marmoset (*Callithrix jacchus*) and black-tufted-ear marmoset (*Callithrix penicillata*). *J Med Primatol* **48**, 32–42.

Baccetti B, Capitani S, Collodel G, Di Cairano G, Gambera L, Moretti E and Piomboni P (2001) Genetic sperm defects and consanguinity. *Hum Reprod* **16**, 1365–71.

Bartoov B, Eltes F, Weissenberg R and Lunenfeld B (1980) Morphological characterization of abnormal human spermatozoa using transmission electron microscopy. *Arch Androl* **5**, 305–22.

Bedford JM and Nicander L (1971) Ultrastructural changes in the acrosome and sperm membranes during maturation of spermatozoa in the testis and epididymis of the rabbit and monkey. *J Anat* **108**, 527–43.

Bezerra LGP, Souza ALP, Silva HVR, Vasconcelos FR, Moura AAA, Pereira AF, Oliveira MF and Silva AR (2018) Ultrastructural description of fresh and frozen/thawed sperm derived from collared peccaries (*Pecari tajacu* Linnaeus, 1758). *Microscop Res Tech* **81**, 1–9.

Bloom E (1973) The ultrastructure of some characteristic sperm defects and a proposal for a new classification of the bull spermogram. *Nord Vet* **25**, 83–91.

Bornens M (2012) The centrosome in cells and organisms. *Science* **335**, 422–26.

Gomendio M and Roldan ER (1991) Sperm competition influences sperm size in mammals. *Proc Biol Sci* **243**, 181–5.

Gould KG (1980) Scanning electron microscopy of the primate sperm. *Int Ver Cytol* **63**, 323–55.

Gould KG and Martin DE (1978) Comparative morphology of primate spermatozoa using scanning electron microscopy. II. Families Cercopithecidae, Lorisidae, Lemuridae. *J Hum Evol* **7**, 637–42.

Humphries S, Evans JP and Simmons LW (2008) Sperm competition: linking form to function. *BMC Evol Biol* **8**, 319.

IUCN (2019) *The IUCN Red List of Threatened Species*. Version 2019-2. http://www.iucnredlist.org. Accessed 20 August 2019.

Leão DL, Miranda AS, Brito AB, Lima JS, Santos RR and Domingues SFS (2015) Efficacious long-term cooling and freezing of *Sapajus apella* semen in ACP-118®. *Anim Reprod Sci* **159**, 118–23.

López-Armengol MF, Jurado SB, Pelufo V and Aisen EG (2012) A quantitative ultramorphological approach for systematic assessment of sperm head regions: an example in rams. *Cryobiology* **64**, 223–34.

Martin DE, Gould KG and Warner H (1975) Comparative morphology of primate spermatozoa using scanning electron microscopy. I. Families Hominidae, Pongidae, Cercopithecidae and Cebidae. *J Hum Evol* **4**, 287–92.

Nakazato C, Yoshizawa M, Isobe K, Kusakabe KT, Kuraishi T, Hattori S, Matsumoto H, Fukui E, Kuwahata A, Ochi M, Kiso Y and Kai C (2015) Morphological characterization of spermatozoa of the night monkey. *J Mamm Ova Res* **31**, 37–40.

Nussdorfer P, Cilenšek I, Zorn B and Petrovič D (2018) Adapted methods for scanning electron microscopy (SEM) in assessment of human sperm morphology. *Bosn J Basic Med Sci* **18**, 43–8.

Oliveira KG, Leão DL, Almeida DVC, Santos RR and Domingues SFS (2015) Seminal characteristics and cryopreservation of sperm from the squirrel monkey, *Saimiri collinsi*. *Theriogenology* **84**, 743–9.

Oliveira KG, Santos RR, Leão DL, Brito AB, Lima JS, Sampaio WV and Domingues SFS (2016a) Cooling and freezing of sperm from captive, free-living and endangered squirrel monkey species. *Cryobiology* **72**, 283–9.

Oliveira KG, Santos RR, Leão DL, Queiroz HL, Paim FP, Vianez-Júnior JLSG and Domingues SFS (2016b) Testicular biometry and semen characteristics in captive and wild squirrel monkey species (*Saimiri* sp.). *Theriogenology* **86**, 879–87.

Ozkavukcu S, Erdemli E, Ayca Isik A, Oztuna D and Karahuseyinoglu S (2008) Effects of cryopreservation on sperm parameters and ultrastructural morphology of human spermatozoa. *J Assist Reprod Genet* **25**, 403–11.

Pesch S, Bostedt H, Failing K and Bergmannc M (2006) Advanced fertility diagnosis in stallion semen using transmission electron microscopy. *Anim Reprod Sci* **91**, 285–98.

Sampaio WV, Oliveira KG, Leão DL, Caldas-Bussiere MC, Queiroz HL, Paim HP, Santos RR and Domingues SFS (2017) Morphologic analysis of sperm from two neotropical primate species: comparisons between the squirrel monkeys *Saimiri collinsi* and *Saimiri vanzolinii*. *Zygote* **25**, 1–8.

Silva HVR, Nunes TGP, Ribeiro LR, Freitas LA, Oliveira MF, Assis Neto AC, Silva AR and Silva LDM (2019) Morphology, morphometry, ultrastructure, and mitochondrial activity of jaguar (*Panthera onca*) sperm. *Anim Reprod Sci* **203**, 84–93.

Sousa PC, Santos EAA, Bezerra JAB, Lima GL, Castelo TS, Fontenele-Neto JD, Silva AR (2013) Morphology, morphometry and ultrastructure of captive six-banded armadillo (*Euphractus sexcinctus*) sperm. *Anim Reprod Sci* **140**, 279–85.

Steinberg ER, Nieves M, Ascunce MS, Palermo AM and Mudry MD (2009) Morphological and genetic characterization of *Saimiri boliviensis*. *Int J Primatol* **30**, 29–41.

Swanson WF, Valle RR, Carvalho FM, Arakaki PR, Rodas-Martínez AZ, Muniz JAPC and García-Herreros M (2016) Sperm morphology assessment in captive neotropical primates. *Reprod Dom Anim* **51**, 623–7.

Visco V, Raffa S, Elia J, Delfino M, Imbrogno N, Torrisi MR and Mazzilli F (2010) Morphological sperm defects analyzed by light microscopy and transmission electron microscopy and their correlation with sperm motility. *Int J Urol* **17**, 259–66.

WHO (2010) *Laboratory Manual for the Examination and Processing of Human Semen*, 5th edn. Geneva, Switzerland: WHO Press.

Zamboni L, Zemjanis R and Stefanini M (1971) The fine structure of monkey and human spermatozoa. *Anat Rec* **169**, 129–53.

https://doi.org/10.1017/S0967199419000868 Published online by Cambridge University Press